European Journal of Pharmaceutics and Biopharmaceutics 119 (2017) 300–309

Contents lists available at ScienceDirect

European Journal of Pharmaceutics and Biopharmaceutics

journal homepage: www.elsevier.com/locate/ejpb

Research paper

Neurotensin receptor 1 facilitates intracellular and transepithelial delivery of macromolecules

Joanna L. Bird [a,1], Rachael Simpson [a], Driton Vllasaliu [b,2], Alan D. Goddard [a,*]

[a] School of Life Sciences, University of Lincoln, Lincoln LN6 7DL, UK
[b] School of Pharmacy, University of Lincoln, Lincoln LN6 7DL, UK

ARTICLE INFO

Article history:
Received 11 January 2017
Revised 2 May 2017
Accepted in revised form 28 June 2017
Available online 6 July 2017

Keywords:
Caco-2
Neurotensin
Neurotensin receptor 1
Peptide-guided drug delivery
Targeted drug delivery

ABSTRACT

G protein-coupled receptors are expressed on the surface of eukaryotic cells and internalise in response to ligand binding. The actions of the hormone and neurotransmitter neurotensin (NT) are predominantly mediated by specific interactions with one such receptor, neurotensin receptor 1 (NTS1), which is upregulated in a variety of cancers, including pancreatic and breast tumours. NTS1 could therefore serve as a target for selective delivery of therapeutics. This study characterised the expression of NTS1 in HEK293 cells, as well as both polarised and non-polarised intestinal epithelial Caco-2 cells. NT-conjugated fluorophores were internalised in NTS1-expressing HEK293 and Caco-2 cells in a receptor-mediated fashion. Confocal microscopy revealed fluorophore localisation in the perinuclear region. Cell uptake and transport across the Caco-2 intestinal model of two NT-conjugated fluorophores (GFP and fluorescein) were compared to evaluate the effect of cargo size on cellular uptake. This work demonstrates that NT ligand conjugation is able to deliver relatively large macromolecular cargoes selectively into cells overexpressing NTS1 and the system is able to effectively translocate macromolecules across an intestinal epithelial model. NTS1 therefore shows potential as a drug delivery target not only for targeted but also non-invasive (oral) delivery of biotherapeutics for cancer.

1. Introduction

Targeted delivery of therapeutics to diseased tissue as a means of increasing the therapeutic benefits of a drug, including reduction of adverse effects [1], is a key aim of modern pharmaceutics. A range of options are available to guide the drug to the cells or tissue of interest, exploiting disease-induced changes in biology as a basis for selectivity. Aberrantly or overexpressed cell-surface receptors offer an attractive route for targeted drug delivery in cancer [2]. Neurotensin (NT) is a tridecapeptide known to exert a variety of effects; it has a dual role as both a neuromodulator in the central nervous system and as a local hormone in the periphery [3]. The actions of NT are mediated by specific interactions with one of three receptors, the first two being G protein-coupled receptors (GPCRs): NTS1, NTS2 and NTS3, all of which are known to internalise upon interaction with NT [4]. NTS1 is thought to play the predominant role in eliciting the actions of NT and is the main focus of this study. NTS1 is known to be upregulated in a variety of different cancer types, including pancreatic and breast tumours [5] and has been demonstrated to be a key driver of cell proliferation, survival, migration and invasion (reviewed in [6]). Indeed, NTS1 antagonists have been proposed as anti-cancer agents, but currently-available drugs exhibit significant toxicity [6].

An alternative approach to the development of such drugs is the use of NTS1 as a molecular target for drug delivery [5–8]. The underpinning theory is that the receptor-ligand-drug complex will internalise, delivering drugs in a targeted manner. Initial studies demonstrated the viability of this approach (reviewed in [6]) and the potential of NT as a drug delivery ligand has been documented recently. Jia et al. [9] investigated the rates of internalisation of NT

Abbreviations: DAPI, 4′,6-diamidino-2-phenylindole; DMEM, Dulbecco's Modified Eagles Medium; DOTA, 1,4,7,10-tetraazacyclododecane-1,4,7,10-tetraacetic acid; F, fluorescein; FBS, foetal bovine serum; F-NT, N-terminally fluorescein-labelled neurotensin; Fluo-NT, fluorescently-labelled neurotensin; GFP, green fluorescent protein; GFP-NT, green fluorescent protein with an N-terminal hexahistidine tag and C-terminal neuroetensin fusion; His_6, hexahistidine tag; His-GFP, green fluorescent protein with an N-terminal hexahistidine tag; HBSS, Hank's Balanced Salt Solution; NT, neurotensin; NTS1, neurotensin receptor 1; NTS2, neurotensin receptor 2; NTS3, neurotensin receptor 3; TEER, transepithelial electrical resistance.

* Corresponding author at: School of Life and Health Sciences, University of Aston, Birmingham B4 7ET, UK.
E-mail address: a.goddard@aston.ac.uk (A.D. Goddard).
[1] School of Biosciences, University of Kent, Canterbury CT2 7NH, UK.
[2] King's College London, Institute of Pharmaceutical Science, London SE1 9NH, UK.

http://dx.doi.org/10.1016/j.ejpb.2017.06.027
0939-6411/

conjugated to 1,4,7,10-tetraazacyclododecane-1,4,7,10-tetraacetic acid (DOTA), used for radiotherapy. This study found that the use of a spacer (β-Alanine) between NT and DOTA increases the internalisation rates of NT analogues, mediated by NTS1, compared to conjugation without a spacer. This reflects the work of Antunes et al. [10] that documents the effect of spacers between somatostatin analogues and radiolabelled DOTA. Other work has used synthetic oligobranched NT conjugates to deliver cargoes to cells, including doxorubicin-loaded liposomes [11] and methotrexate or gemcitabine [12], as well as oligobranched NT derivatives to target NT receptors [12–14]. However, little is known of the molecular mechanism underpinning NTS1 internalisation or the limitations on the size and nature of cargo which can be delivered. This is of increasing importance as many recently-developed anticancer therapeutics are biologics.

NT provides a suitable ligand for targeted delivery as it interacts with the NTS1 receptor with high affinity (K_d 0.3–1 nM) [15] and only its six C-terminal amino acids are required for receptor binding [16], which allows covalent or translational attachment of a variety of macromolecules to the N-terminus. In most cell types, receptor-mediated peptide internalisation results in fusion with lysosomes and degradation [17]. However, internalisation of NT has been shown to follow a different route. Vandenbulcke et al. investigated the method of internalisation of fluorescently labelled NT (Fluo-NT) in COS-7 cells transfected with NTS1 and demonstrated, by methods of pathway-selective inhibition (hypertonic sucrose, potassium depletion and cytosol acidification), that NT internalisation is mediated by clathrin coated pits [18]. Importantly, NT and NTS1 appear to separate on internalisation and Fluo-NT was demonstrated to traffic to the transgolgi network [18]. This provides a possible lysosome-escape route for macromolecules tagged with NT, mitigating lysosome degradation as one of the key problems of intracellular drug delivery. This makes the NT/NTS1 cell entry pathway a particularly attractive option for therapeutic delivery. However, NT also has a short serum half-life (minutes) but this can be mitigated by modifications to the peptide [19,20]. In this study, we have focussed on native NT as proof of concept due to its well-characterised biological action and the ease of producing NT-macromolecule complexes. This allows us to characterise the properties of NTS1 internalisation, but future translational work should focus on stable analogues.

Here, we demonstrate that NTS1 can be used to internalise payloads of different sizes, namely a relatively small fluorophore or macromolecular GFP. Efficient internalisation of these cargoes is observed in HEK293 cells expressing NTS1 and this uptake is significantly attenuated via competition with either receptor agonists or antagonists. Importantly, we demonstrated efficient uptake into, and transport across, an intestinal epithelial model consisting of polarised Caco-2 monolayers, which endogenously express NTS1. This study demonstrates for the first time that in addition to its potential as a targeting moiety for efficient and receptor-mediated uptake of macromolecules specifically into cells expressing or overexpressing its receptor(s) (e.g. cancer), NT is also able to ferry the cargo transintestinally in a receptor-mediated fashion, hence also demonstrating potential for oral delivery of macromolecules. This addresses a significant challenge in the field [21].

2. Materials and methods

2.1. Materials

Caco-2 cells were obtained from the European Collection of Cell Cultures (ECACC) and were used between passages 60–80. HEK293 cells were obtained from the American Type Culture Collection (ATCC) and were used between passages 25–40. Dulbecco's Modified Eagles Medium (DMEM; with 4500 mg/L glucose, L-glutamine, sodium pyruvate and sodium bicarbonate), Hank's Balanced Salt Solution (HBSS; with sodium bicarbonate and without phenol red), Trypsin/EDTA solution (0.25% trypsin, 0.02% EDTA), antibiotic/antimycotic solution (penicillin, streptomycin and amphotericin), foetal bovine serum (FBS, non-USA origin), dimethylsulphoxide (DMSO), trypan blue solution (0.4% solution) and poly-l-lysine (0.1% solution, mw = 70,000–15,000) were all obtained from Sigma Aldrich (UK). DMEM was supplemented with 10% FBS and 1% antibiotic/antimycotic solution to produce complete DMEM. Transwell® permeable supports of 12 mm diameter and 0.4 μm pore size (polyester membrane) were obtained form Corning Life Sciences (USA). Human neurotensin was supplied by Sigma Aldrich and SR142948 (non-peptide NTS1 and NTS2 receptor antagonist) were obtained from Tocris Bioscience© (UK). Protease inhibitor tablets (cOmplete™ protease inhibitor cocktail tablets, EDTA-free) were supplied by Roche Diagnostics (USA).

2.2. Methods

2.2.1. GFP-NT and GFP synthesis

A translational fusion of His-GFP and NT was produced by sequential PCR (AG1 and AG3, AG2 and AG4, AG2 and AG5) on a clone of Emerald GFP to extend the C-terminus to encode NT and the N-terminus to encode a His_6 tag. The primers used are illustrated in Table 1. The final PCR product was digested with *Nde*I/*Bam*HI and cloned into *Nde*I/*Bam*HI digested pET17 b. pET17 b-GFP was produced by Quikchange mutagenesis using primers AG6 and AG7 to introduce a stop codon prior to the NT coding sequence in pET17b-GFP-NT. GFP-NT and GFP were produced by recombinant expression in *E. coli* BL21(DE3) grown in LB broth containing 100 μg/ml ampicillin, followed by cell lysis using pulsed sonication (5 min, 5 s on, 5 s off) in 50 mM Tris, 100 mM NaCl pH7.4 at 2 ml per litre of culture. Purification was achieved via Immobilised Metal Affinity Chromatography using 1 ml HisTrap HP columns (GE Healthcare Life Sciences). Briefly, the column was equilibrated with 5 column volumes (CV) 50 mM Tris, 100 mM NaCl pH7.4 followed by sample loading. The column was then washed with 10 CV of the same buffer also containing 50 mM imidazole. Proteins were eluted using the same buffer containing 200 mM imidazole. Protein purity was assessed via SDS-PAGE and quantitated via UV–Vis spectrophotometry. All proteins used were >95% pure.

2.2.2. Cell culture

Caco-2 and HEK293 cell lines were routinely cultured in 75 cm^2 flasks at 5% CO_2, 95% relative humidity and 37 °C in DMEM. Caco-2 cells were seeded on Transwell® filter at a seeding density of 1×10^5 per well and cultured for 21–24 days, with medium replacement every two days. Transepithelial Electrical Resistance (TEER) was measured to monitor Caco-2 cell growth, polarisation and cell monolayer integrity. HEK293 cells are weakly adherent and were therefore cultured on poly-l-lysine (0.1% w/v) coated coverslips in 12-well plates.

2.2.3. HEK293. transfection

HEK293 cells cultured in 12-well plates were transfected using Lipofectamine® 2000 Transfection reagent and the NTS1 containing plasmid (pcDNA3.1-NTS1, cDNA.org). This procedure used 4 μl Lipofectamine and 1 μg DNA per well. Lipofectamine and DNA (in medium) were incubated at room temperature for 60 min to form DNA-containing liposomes. Cell medium was replaced with reduced serum media (5% FBS) and the transfection mixture was then applied, followed by cell incubation at 5% CO_2, 95% relative humidity and 37 °C for 24 h before use in experiments.

Table 1
Oligonucleotide primer sequences used in this study. Primers are displayed 5′ to 3′ and lowercase nucleotides indicate those which are not complementary to the template sequence.

Primer name	Sequence
AG1	caccatcaccatcacATGGTGAGCAAGGGCGAGGAGCTG
AG2	ggggggcatatgcatcaccatcaccatcac
AG3	gttttcatacagttcCTTGTACAGCTCGTCCATGCC
AG4	tataacgacgcggtttgttttcatacagttcCTTGTACAGC
AG5	ccggatccttacagaatataacgacgcggtttg
AG6	GGACGAGCTGTACAAGTAAgaactgtatgaaaacaaacc
AG7	ggtttgttttcatacagttcTTACTTGTACAGCTCGTCC

2.2.4. Immunostaining

Caco-2 cells were cultured on Transwell® permeable inserts for 21 days and evaluated for monolayer integrity by TEER measurements. Cell monolayers were fixed with 4% w/v paraformaldehyde in PBS and washed 3 times with PBS. Cells were then incubated for one hour with 1% w/v bovine serum albumin (BSA) in PBS at room temperature as a non-specific binding blocking step. A 1:5000 dilution of the primary antibody (Rabbit Anti-Human NTS1; Sigma Aldrich (UK)) was prepared in 1% w/v BSA in PBS, as recommended by the supplier, and applied to fixed cell monolayers for one hour at room temperature. Primary antibody solution was omitted for the negative controls and cells were incubated with the antibody diluent solution (BSA). Each monolayer was then washed thoroughly with PBS and incubated for one hour with goat, anti-rabbit AlexaFluor®488 at 1:800 dilution in 1% w/v BSA/PBS. The secondary antibody solution was then removed and cells washed extensively with PBS. Filter inserts were then excised and mounted on a glass slide, treating with Fluoroshield™ with DAPI mounting medium (Sigma Aldrich (UK)).

Caco-2 cells were also immunostained as per the method above in their undifferentiated state, following growth on 12-well plates. Similarly, HEK293 immunostaining was conducted after culture on 12-well plates. Confocal microscopy imaging was performed using a Leica TCS SP8 confocal microscope using constant laser gain for DAPI and AlexaFluor®488 in all immunostained sections. Where indicated, cells were permeabilised by addition of 0.1% Triton X 100 in PBS for 20 min at room temperature, in sterile conditions.

2.2.5. Cell uptake studies

Cell uptake studies were performed in 12-well plates for undifferentiated Caco-2 and HEK293 cells following 48-h culture and in Transwell® permeable inserts for polarised and differentiated Caco-2 monolayers. For the latter, cells were cultured on Transwell® filter inserts for 21–24 days and TEER measured before uptake studies to confirm cell monolayer polarity and integrity (typically ~2000 Ωcm^2) [22]. In both cases, cells were initially incubated with HBSS for at least 30 min. Samples of GFP-NT, with or without NT, SR142948, or GFP were prepared in HBSS and applied to the cells (apical side in case of differentiated, 21-day filter culture Caco-2 cell monolayers). Cells were incubated with the samples for different periods between 30 min and 2.5 h. Thereafter, samples were removed and cells washed with cold PBS, followed by cell permeabilisation using 200 µl of 0.1% v/v Triton X-100 in protein buffer (200 mM Tris, 50 mM NaCl with 200 µl of 1x protease inhibitor stock solution; 30 min incubation). Samples were then centrifuged at 17,900*g* and supernatant quantified by fluorescence measurements using a Tecan Infinite® Pro 200 microplate reader (Fluorescein excitation 490 nm, emission 525 nm; GFP excitation 488 nm, emission 509 nm).

2.2.6. Caco-2. monolayer transport studies

Differentiated Caco-2 monolayers (21-day filter culture) were equilibrated in HBSS for at least 30 min. Cell monolayer TEER was measured (in HBSS) prior to the transport study to ensure cell monolayer integrity (typically ~2000 Ωcm^2; cells with TEER < 1000 Ωcm^2.were excluded from the study). GFP-NT (with

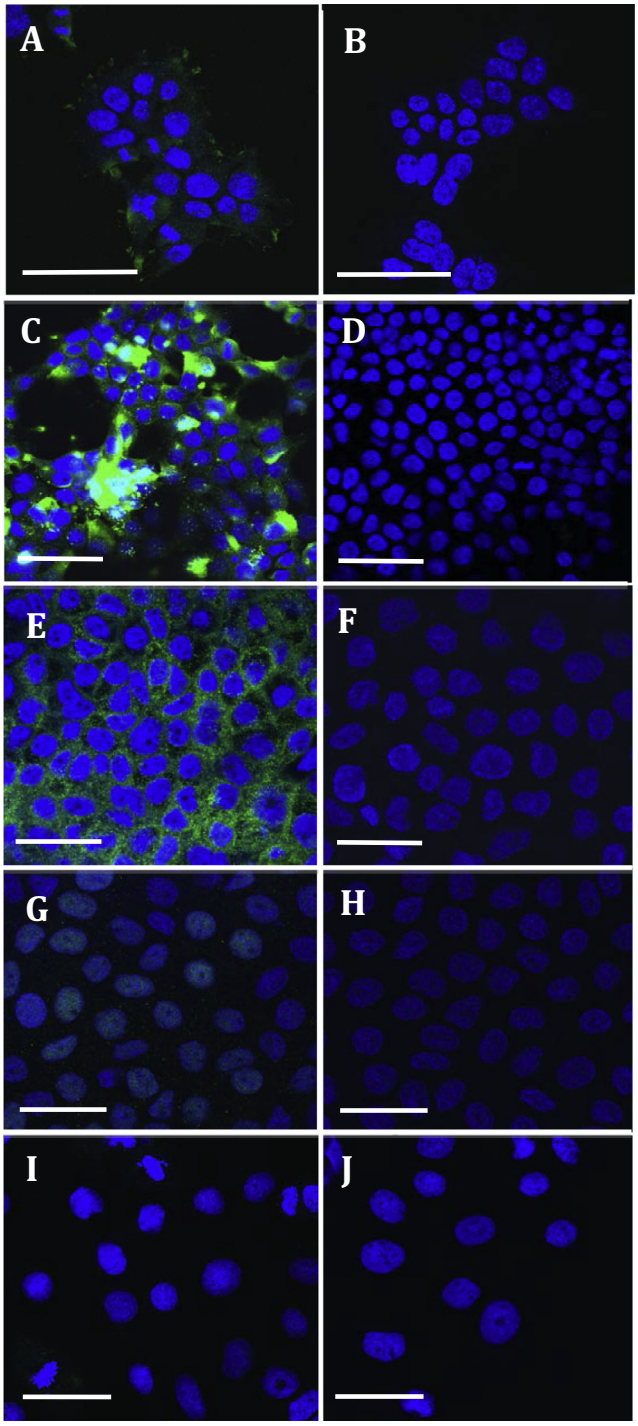

Fig. 1. Neurotensin 1 (NTS1) receptor immunostaining in HEK293 and Caco-2 cells. (A) Non-transfected HEK293 cells and negative control where cell treatment with primary anti-NTS1 antibody was omitted (B). (C) HEK293 cells transfected with 4 µl Lipofectamine and negative control (D). (E) Non-permeabilised, differentiated (21-day filter culture) Caco-2 cells and negative control (F). (G) Permeabilised, differentiated (21-day filter culture) Caco-2 cells and negative control (H). (I) Undifferentiated (2-day plastic culture) Caco-2 cells and negative control (J). Blue staining represents cell nuclei (stained by DAPI) and green staining represents NTS1. Immunostaining performed using rabbit, anti-human NTS1 primary antibody and goat, anti-rabbit AlexaFluor®488 secondary antibody. Scale bar = 50 µm. (For interpretation of the references to colour in this figure legend, the reader is referred to the web version of this article.)

or without inhibitors NT and SR142948) or GFP were prepared at different concentrations in HBSS and applied to the apical side of the cell monolayers. A 100 μl sample of HBSS from the basal side of the Transwell® was taken immediately after introduction of the samples as a measure of protein transport through the monolayer at time 0 min. 100 μl samples were then taken every 30 min for three hours, replacing the volume of sample taken with fresh HBSS each time. The effective dilution was accounted for when calculating concentrations. Between samples, the Transwell® plate was returned to the incubator. Protein transport was quantified using fluorescence as described above. TEER was measured following the transport study to ensure cell monolayer integrity was intact.

2.2.7. Statistical analysis

The parametric unpaired Students t-test was used to determine statistical significance with Welsh's correction to correct for small data sets.

3. Results

Initial experiments focussed on characterisation of NTS1 receptor expression in HEK293 and Caco-2 cells. HEK293 cells were chosen as a widely-used tumourigenic model [23] and Caco-2 cells represent the classic epithelial gut model [24]. Fig. 1 shows confocal micrographs of non-transfected HEK293 cells (A and B); transfected HEK293 cells (C and D); non-permeabilised, differentiated (21-day filter culture) Caco-2 cells (E and F), permeabilised, differentiated Caco-2 cells (G and H) and undifferentiated (2-day plastic culture) Caco-2 cells (I and J). A negative control where cell treatment with the primary antibody was omitted is shown in each scenario. The data demonstrates a higher level of NTS1 expression in transfected HEK293 cells (Fig. 1C) than non-transfected HEK293 (Fig. 1A) and non-permeabilised, differentiated Caco-2 monolayers (Fig. 1E). Dramatically reduced NTS1 expression is apparent in permeabilised, differentiated Caco-2 monolayers (Fig. 1G) compared to non-permeabilised counterparts. Non-differentiated Caco-2 cells do not express detectable levels of NTS1 (Fig. 1I). We observed qualitatively higher levels of NTS1 expression on the apical surface of the differentiated Caco-2 monolayer compared to the basal surface (Fig. 2).

F-NT uptake by non-transfected and transfected HEK293 cells is shown Fig. 3, both quantitatively by fluorimetry and qualitatively by confocal microscopy. Cells were treated with F-NT alone or in the presence of excess free NT or excess SR142948. Free NT competitively inhibits all NT receptors, and SR142948 selectively inhibits NTS1 and NTS2. The data shows that the uptake of F-NT alone is greater in transfected HEK293 cells ($p = 0.026$; Fig. 3B) compared to non-transfected cells (Fig. 3A), suggesting that uptake correlates with NTS1 expression. F-NT uptake is notably higher relative to unconjugated fluorescein. Cell internalisation of F-NT is also dramatically reduced by the co-application of excess free NT (also shown by confocal microscopy in Fig. 3C and D) or SR142948.

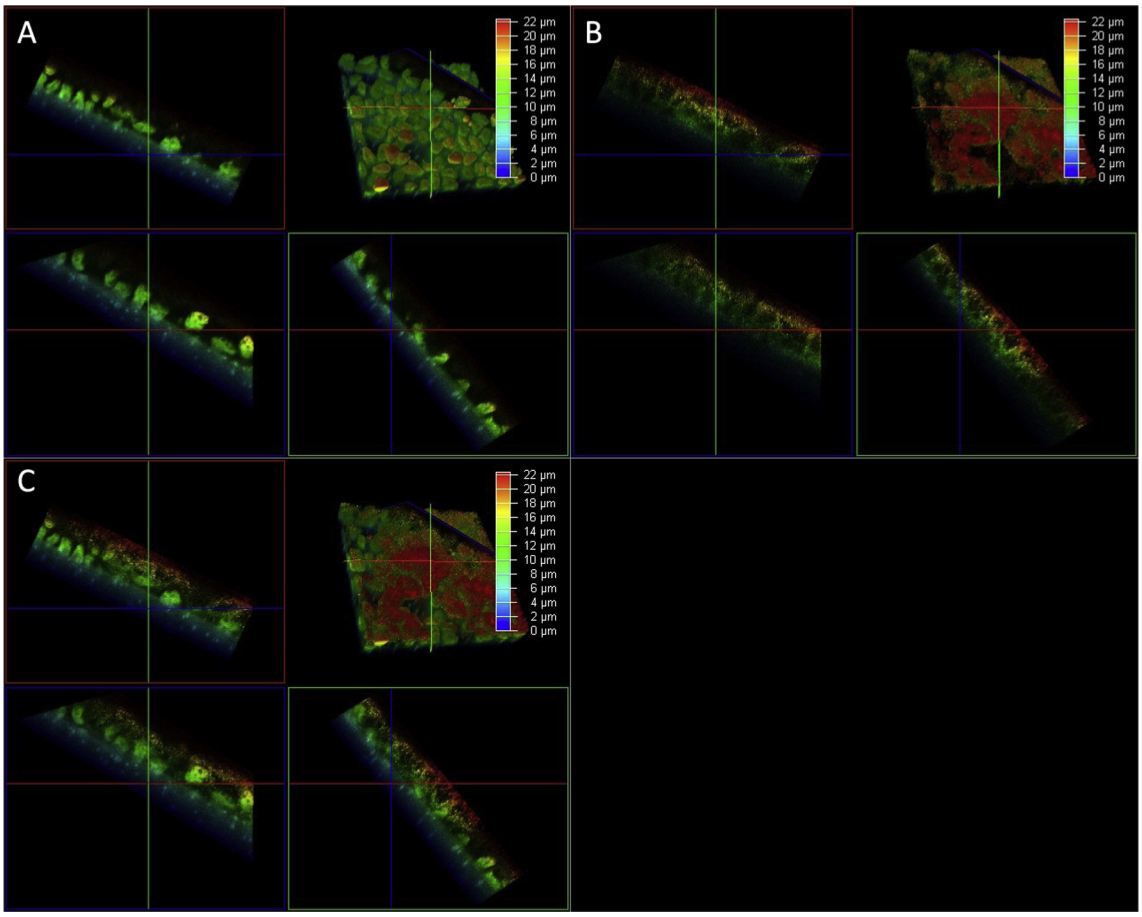

Fig. 2. Neurotensin 1 (NTS1) receptor immunostaining in differentiated Caco-2 cell monolayers (21-day filter culture). (A) DAPI-stained with false-colour imaging indicating depth relative to the surface of the Transwell plate (0 μm) (B). Anti-NTS1-immonstained Caco-2 monolayer with false-colour imaging indicating depth relative to the surface of the Transwell plate (0 μm). Immunostaining performed using rabbit, anti-human NTS1 primary antibody and goat, anti-rabbit AlexaFluor®488 secondary antibody. (C) Overlay of images in panels A and B.

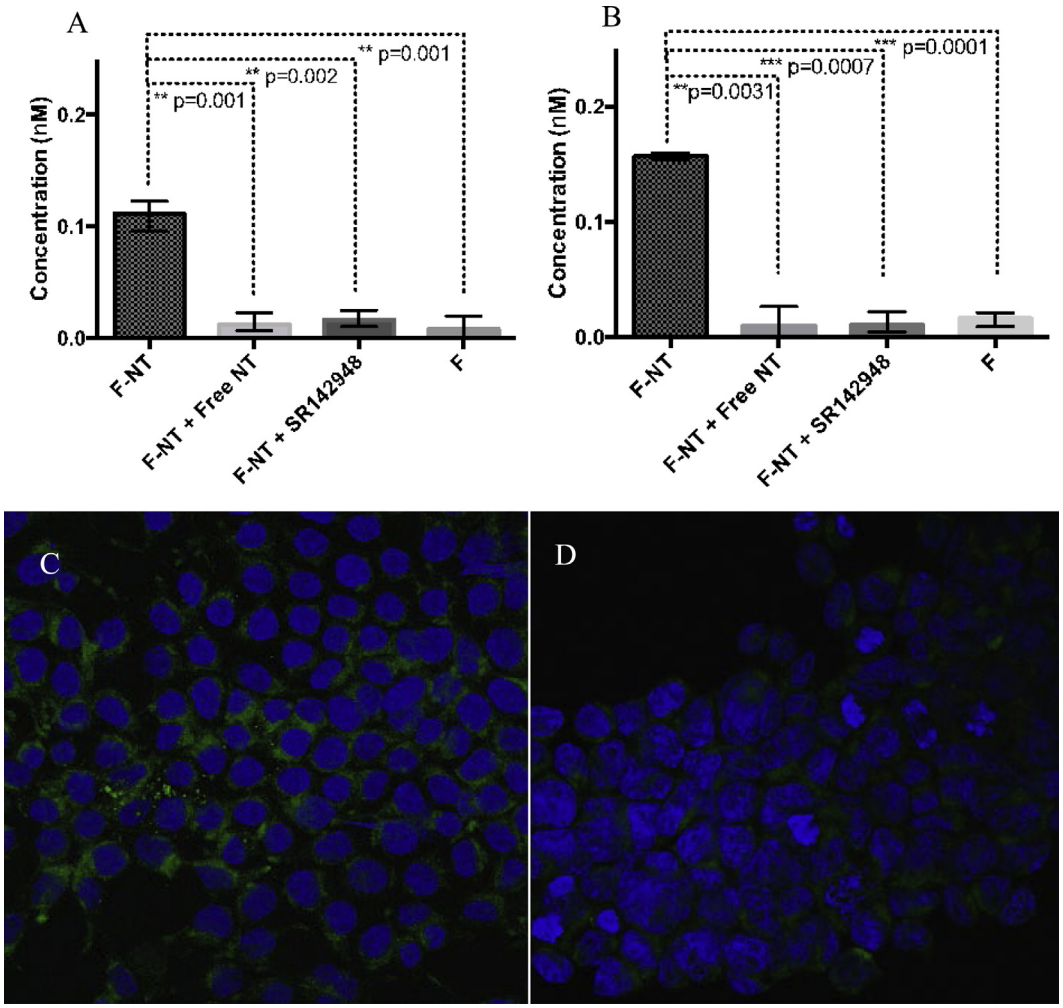

Fig. 3. Internalisation of NT-conjugated fluorescein in non-transfected and transfected HEK293 cells. Quantification of F-NT uptake in (A) non-transfected and (B) pcDNA3.1-NTS1 transfected HEK293 cells. 'F-NT' denotes application of F-NT at 20 nM; 'F-NT + Free NT' denotes application of 20 nM NT-F with 2 μM free neurotensin; 'F-NT + SR142948' denotes application of 20 nM F-NT with 200 nM SR142948; 'F' denotes application of fluorescein at 20 nM. Error bars are representative of mean ± SD and each data point, n = 3. Confocal microscopy images of pcDNA3.1-NTS1 transfected HEK293 after (C) incubation with 20 nM F-NT for 1 h and (D) incubation with 20 nM F-NT and 2 μM NT for 1 h. Scale bar = 50 μm.

GFP-NT uptake by non-transfected and transfected HEK293 cells is shown Fig. 4. Cell uptake of GFP alone was also tested in these studies to establish the levels of internalisation of GFP itself and confirm whether cell uptake of GFP-NT is mediated by NT. The data shows a similar pattern in non-transfected (Fig. 4A) and transfected cells (Fig. 4B), with GFP-NT showing a higher uptake compared to GFP and also in conditions where GFP-NT was applied alone (without excess free NT or SR142948). However, the difference between these conditions in non-transfected cells was not statistically significant while in transfected HEK293 cells this difference was statistically significant ($p < 0.01$), suggesting correlation with relative NTS1 expression. Fig. 4C and D depict confocal micrographs comparing transfected HEK293 cells treated with GFP-NT or GFP-NT plus a 100x excess of NT. Fluorescence due to GFP-NT was observed in areas localised around the nucleus in cells treated with GFP-NT only and notably lower levels of fluorescence signal were apparent in cell samples exposed to excess NT.

NT-conjugated fluorophore internalisation in undifferentiated Caco-2 cells is shown in Fig. 5. Caco-2 cells were incubated with F-NT (Fig. 5A) or GFP-NT (Fig. 5B) alone, GFP-NT or F-NT with excess free NT or excess free SR142948. Cell uptake behaviour of fluorophores alone was also performed to provide a comparison with the internalisation of NT-conjugated equivalent. Cell uptake of both NT-fluorophores is not affected by competitive NTS receptor inhibition via free NT or excess free SR142948. The extent of internalisation seen for each condition is comparable to the uptake of fluorophore alone. Confocal micrographs showing this uptake are shown in Fig. 5C and 5D for F-NT and GFP-NT, respectively (applied without competitive inhibitors). The images show minimal F-NT fluorescence (green) within the cells, suggesting limited uptake in undifferentiated Caco-2 cells.

Cell uptake of NT-conjugated fluorophores into polarised, differentiated Caco-2 monolayers is shown in Fig. 6. NT-conjugated fluorophore (F-NT – Fig. 6A and GFP-NT – Fig. 6B) uptake after 150 min is notably higher compared to the internalisation in the presence of excess free NT, as well as the unconjugated fluorophores. Importantly, NT-conjugated fluorophore uptake in polarised Caco-2 cells is markedly greater to that in undifferentiated cells (Fig. 5). This uptake is quantified by measurements at 30-min intervals for a total of 150 min (Fig. 6C and D). F-NT uptake increases with incubation time up to 60 min, with a plateau apparent at subsequent time points. GFP-NT entry into cells mirrors the pattern observed with F-NT.

Following the demonstration that NT-conjugated fluorophores are capable of internalisation in polarised Caco-2 cells, we further probed whether these molecules are able to traverse polarised

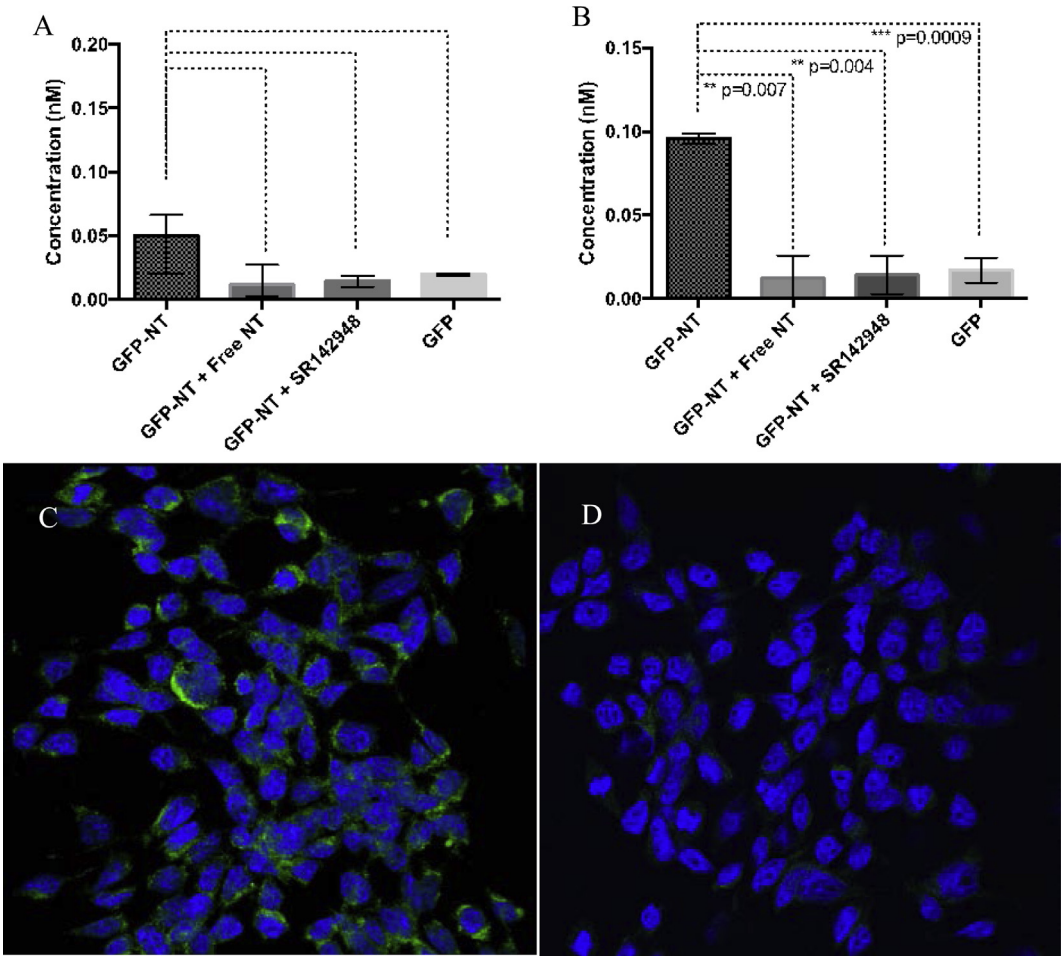

Fig. 4. Internalisation of NT-conjugated GFP in non-transfected and transfected HEK293 cells. Quantification of GFP-NT uptake in (A) non-transfected and (B) pcDNA3.1-NTS1 transfected HEK293 cells. 'GFP-NT' denotes application of GFP-NT at 20 nM; 'GFP-NT + Free NT' denotes application of 20 nM GFP-F with 2 μM free neurotensin; 'GFP-NT + SR142948' denotes application of 20 nM GFP-NT with 200 nM SR142948; 'GFP' denotes application of GFP at 20 nM. Error bars are representative of mean ± SD and each data point, n = 3. Confocal microscopy images of pcDNA3.1-NTS1 transfected HEK293 after (C) incubation with 20 nM GFP-NT for 1 h and (D) incubation with 20 nM GFP-NT and 2 μM NT for 1 h. Scale bar = 50 μm.

Caco-2 monolayers, as a way of assessing the potential of NT-NTS1 to act as a system capable of ferrying therapeutics across the intestinal epithelium. Fig. 7 shows the apical-to-basolateral transport of F-NT and GFP-NT in Caco-2 monolayers, with samples quantified at 30-min intervals in a 180-min study. The data shows that both F-NT (Fig. 7A) and GFP-NT (Fig. 7B) traverse Caco-2 monolayers significantly more efficiently than the respective unconjugated fluorophores. With both F-NT and GFP-NT a concentration-dependent effect is observed, with higher concentrations demonstrating larger levels of transport, as well as process saturation with time. Another important observation to note when comparing Fig. 7A and B is that F-NT translocated across polarised Caco-2 monolayers at markedly higher levels than GFP-NT.

4. Discussion

This work assessed whether a receptor demonstrated to exhibit differential expression in cancerous cells can be considered as a system that offers both targeted drug delivery to cancer and means of enhancing macromolecular absorption across the gut epithelium following oral administration. We utilised both transfected and non-transfected HEK293 cells, as well as Caco-2 intestinal epithelial cells as systems with different NTS1 expression profiles. Expression of NTS1 in HEK293 cells is consistent with previous studies [25]. NT also acts as a local hormone in the gut [3] and hence NTS1 expression in intestinal epithelial cells is neither unexpected nor non-physiological [26,27]. Examining the expression of NTS1 in transfected HEK293 cells, confocal micrographs reveal high levels of positive fluorescence signal in cells immunostained for NTS1 receptor (Fig. 1C). Work also showed that differentiated, polarised Caco-2 monolayers express the NTS1 receptor (Fig. 1E). Dramatically reduced NTS1 expression was observed following detergent-mediated permeabilisation (Fig. 1G), which suggests predominant NTS1 localisation in the plasma membrane rather than intracellular membranes. We also show that the expression of the NTS1 receptor in non-differentiated Caco-2 cells is undetectable (Fig. 1I). It is not completely clear why Caco-2 cells exhibit differentiation-dependent expression of NTS1 but these findings correlate with observations that NT expression is increased in cells of the villi compared to those in the crypts [28]. Differentiated Caco-2 cells are a model of villi enterocytes and hence expression of a cognate receptor for NT aligns with the role in gastric function [28]. Additionally, similar findings have been reported previously for the class B type I scavenger receptor (SR-BI) [29] and vitamin B2 (riboflavin) transporters [30].

Comparing NT-fluorophore uptake behaviour in non-transfected and transfected HEK293 cells (Figs. 3 and 4), the data reveal that cell uptake levels of F-NT or GFP-NT alone are significantly greater in transfected HEK293 cells compared to

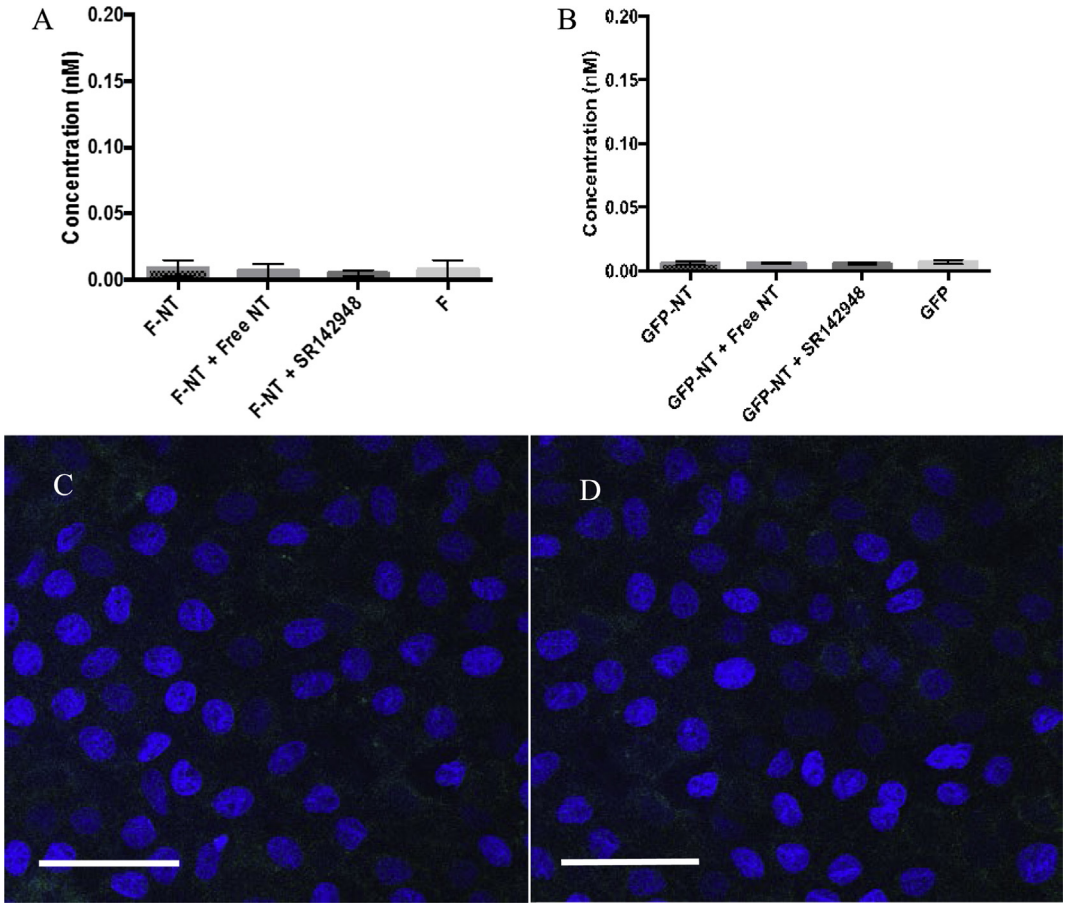

Fig. 5. Uptake of NT-conjugated fluorophores in undifferentiated (2-day plastic culture) Caco-2 cells. Quantification of cell internalisation of (A) F-NT and (B) GFP-NT. 'F-NT' denotes application of 20 nM F-NT, 'F-NT + Free NT' denotes application of 20 nM F-NT with 2 μM free NT, 'F-NT + SR142948' denotes application of 20 nM F-NT with 200 nM SR142948, 'F' denotes application of 20 nM Fluorescein. 'GFP-NT' denotes application of 20 nM GFP-NT, 'GFP-NT + Free NT' denotes application of 20 nM GFP-NT with 2 μM free NT, 'GFP-NT + SR142948' denotes application of 20 nM GFP-NT with 200 nM SR142948, 'GFP' denotes application of 20 nM GFP. Error bars are representative of mean ± SD,n = 3. (C) Confocal micrograph showing F-NT internalisation after incubation with 20 nM F-NT for 1 h. (D) GFP-NT internalisation following incubation with 20 nM GFP-NT for 1hr. Scale bar = 50 μm.

non-transfected cells. Although it may be expected that uptake was even higher in transfected cells, it is likely that a cellular process downstream of ligand-receptor interactions reaches saturation e.g. receptor internalisation. Uptake of NT-conjugated fluorophores was rapid before eventual saturation. NTS1 appears to be degraded following internalisation [18] and is regenerated on the cell surface via *de novo* synthesis [5]. Although precise measurements of NTS1 expression in native tissue have not been reported, GPCR levels on the cell surface are typically in the order of 1×10^3–1×10^4 molecules/cell. Therefore, sufficient uptake of NT-conjugated molecules is potentially possible to enable delivery of macromolecules to therapeutically sufficient levels, especially considering the large surface area of the intestinal epithelium. Although limited expression of other neurotensin-binding receptors may occur in the cell models used, the increases in uptake observed following NTS1 overexpression confirm that this receptor is a viable target for drug uptake; it has been demonstrated that NTS2 expression is undetectable in HEK293 cells [25]. Competitive NTS1 receptor inhibition with excess free NT or excess SR142948 produced a clear inhibition of uptake in both transfected and non-transfected HEK293 cells, while with GFP-NT this inhibition was only apparent in transfected HEK293 (a statistically significant inhibition was not apparent in non-transfected HEK293 cells, although qualitative differences are evident). Inhibition of uptake by excess ligand in transfected HEK293 cells was also confirmed by confocal microscopy. These data therefore point to NTS1 receptor-mediated uptake of NT-conjugated fluorophores in transfected HEK293 cells. The competitive inhibition by NT and SR142948 of uptake of NT-conjugated fluorophores is likely to be bimodal. Firstly, a direct steric competition at the NT-binding site of NTS1 [15] and, secondly, receptor internalisation which removes receptors from the cell surface [5].

NT-conjugated fluorophore internalisation by undifferentiated Caco-2 cells is limited (as shown both quantitatively and by confocal microscopy in Fig. 5) and comparable to the uptake of fluorophore alone. Furthermore, competitive receptor inhibition did not achieve a reduction in NT-conjugated fluorophore uptake in undifferentiated Caco-2 cells. These data collectively imply that in undifferentiated Caco-2 cells any entry of NT-conjugated fluorophores is limited and takes place via a mechanism other than NTS receptor mediated internalisation. This is in line with the finding that NTS1 expression was below detectable limits in undifferentiated Caco-2 cells, confirming the system's ability to specifically delivery therapeutic payloads predominantly in cells expressing NTS1 receptor. On the other hand, polarised Caco-2 monolayers demonstrated uptake of both NT-conjugated fluorophores (F-NT and GFP-NT; Fig. 6), at significantly higher levels compared to that in undifferentiated cells and the unconjugated fluorophores and the internalisation of NT-conjugated fluorophores is markedly reduced following competitive receptor inhibition. Differentiated, polarised Caco-2 monolayers, which unlike non-differentiated counterparts clearly express NTS1, are therefore

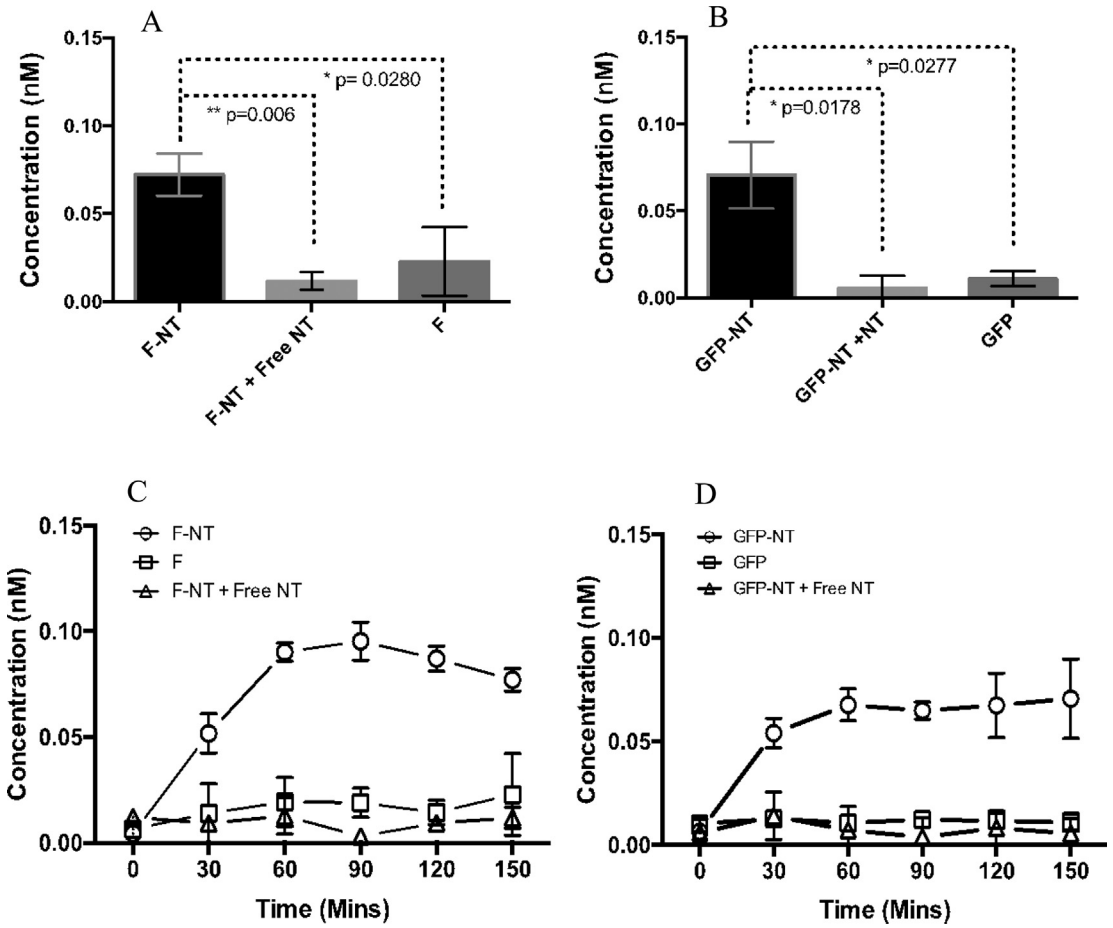

Fig. 6. Uptake of NT-conjugated fluorophores in differentiated Caco-2 cell monolayer (21-day filter culture). Quantification of cell internalisation of (A) F-NT and (B) GFP-NT 150 mins after fluorophore application. Time-dependent uptake of NT-conjugated fluorophores (C) F-NT and (D) GFP-NT. 'F-NT' denotes application of 100 nM F-NT, 'F-NT + Free NT' denotes application of 100 nM F-NT with 10 μM free NT, 'F' denotes application of 100 nM Fluorescein. 'GFP-NT' denotes application of 100 nM GFP-NT, 'GFP-NT + Free NT' denotes application of 100 nM GFP-NT with 10 μM free NT, 'GFP' denotes application of 100 nM GFP. Data points are representative of the mean of n = 3 independent experiments and error bars are representative of ± standard deviation (SD).

capable of internalising NT fluorophores via the NTS1 receptor. Significant uptake of NT-conjugated fluorophores was observed at 100 nM extracellular concentration. This is consistent with other studies in which branched NT-conjugated drugs have EC_{50} values in the range of 100–400 nM [8]. Low levels of free fluorescein uptake observed here are consistent with other studies, with the applied concentration being significantly lower than the observed Km for uptake into Caco-2 cells of 7.7 mM [31].

Following the demonstration that in differentiated Caco-2 monolayers NT-conjugated fluorophores internalise through receptor-mediated endocytosis, subsequent work established whether NT-conjugated fluorophores have the capacity to translocate across intestinal polarised monolayers, which, to our knowledge, is the first time that neurotensin has been investigated for such purpose. To achieve successful systemic drug delivery through the gastrointestinal mucosa, the therapeutic must be effectively internalised into epithelial cells from the gastrointestinal lumen and released at the basal side. Owing to their physicochemical characteristics (molecular size), NT-conjugated fluorophores are not expected to be absorbed across the epithelium by diffusion/partitioning into epithelial membranes. Rather, macromolecules generally traverse the epithelium by transcytosis (paracellular space is considered inadequate for molecules over 1000 Da). Following internalisation into epithelial cells, the fate of the cargo is dependent on the cell sorting machinery, with the material most likely undergoing a mixture of recycling, delivery to late endosomes and lysosomes, or transcytosis. Fig. 7 shows that both F-NT and GFP-NT traverse differentiated Caco-2 monolayers significantly more efficiently than the respective unconjugated fluorophores and in a concentration-dependent manner. Transport process saturation was apparent, similarly to the previously reported behaviour of IgG in airway epithelial monolayers [32]. This likely correlates with the internalisation of NT receptors, which is an established desensitisation mechanism for GPCRs. Notably, F-NT transport across differentiated Caco-2 monolayers was markedly higher than GFP-NT, which suggests an effect by the size of the cargo conjugated to NT. Given previous data [18] it is also possible that the NT-conjugated cargoes will escape the lysosomal pathway, increasing the likelihood of effective drug delivery. Although NT receptors are expressed in the brain, it is likely that many of the NT-macromolecular drug fusions will be too large to cross the blood-brain barrier, thus eliminating a potentially significant off-target effect.

In order to best leverage NTS1 as a drug targeting system, it is highly desirable to have a comprehensive understanding of its cargo limitations and intracellular trafficking. Overall, this work indicates efficient and receptor expression-dependent uptake of NT-conjugated fluorophores by HEK293 and Caco-2 cells, with NTS1 demonstrating potential for uptake of a range of molecular weight therapeutics following oral administration. The size dependence of the cargo is clear, but it is still possible to deliver relatively large macromolecules (GFP has a molecular weight of

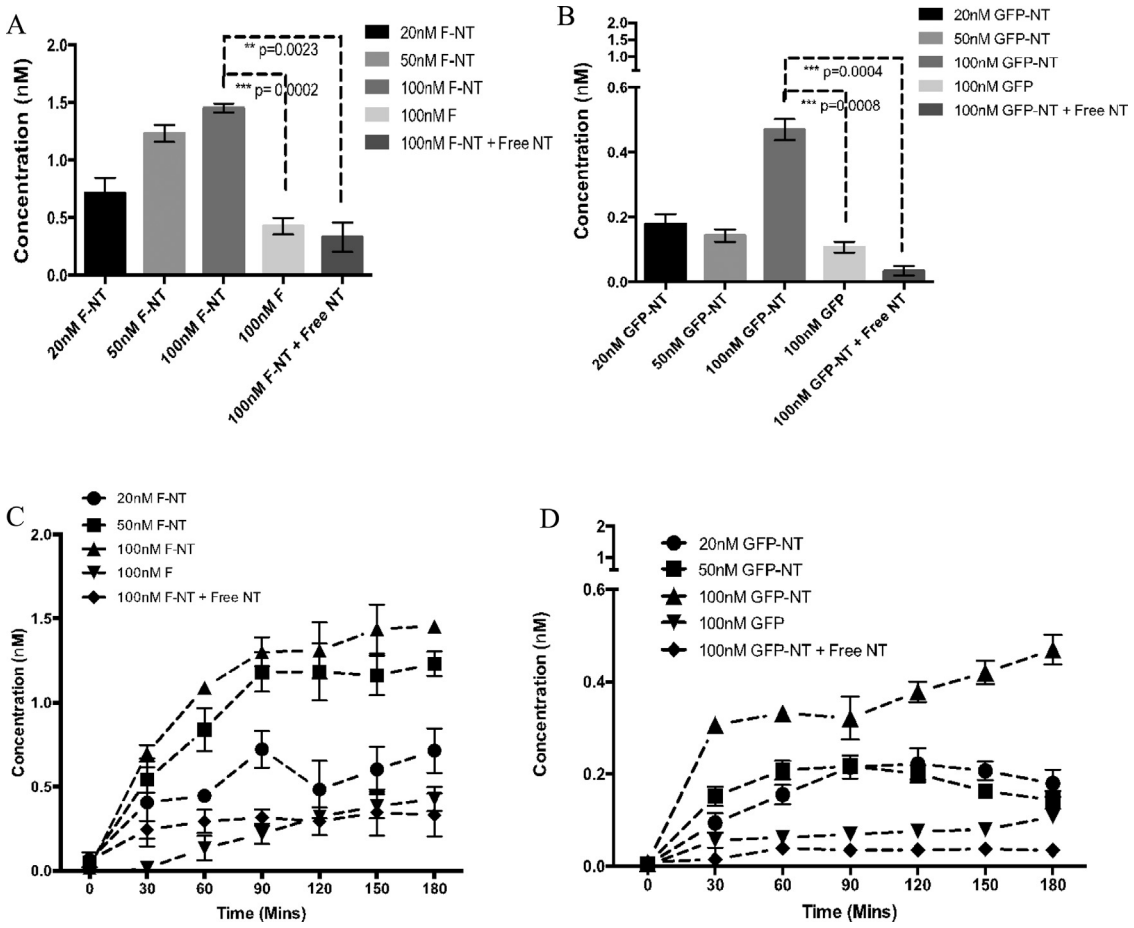

Fig. 7. Apical-to-basolateral transport of NT-conjugated fluorophores in differentiated Caco-2 cell monolayer (21-day filter culture). (A) Transport of F-NT following application at 20 nM, 50 nM or 100 nM F-NT alone or in combination with 100x free NT to the apical side of the monolayers. 100 nM F alone was used as a negative control. Transport was measured after 180 min. (B) Transport of GFP-NT following application at 100 nM, 500 nM or 1 μM alone or combination 100 nM GFP-NT + 100x excess free NT to the apical side of the monolayers. 1 μM GFP alone was used as a negative control. Transport was measured after 180 min. (C) Time course of F-NT transport as described in (A). (D) Time course of GFP-NT transport as described in (B). Data points are representative of the mean of n = 3 independent experiments and error bars are representative of ± SD.

27 kDa). It is also likely that these findings are translatable to other GPCRs assuming a common internalisation mechanism. Further work will focus on characterising the method of internalisation, specifically whether drug-ligand conjugates utilise a different internalisation pathway to the ligand alone, as found with B_{12}-conjugated nanoparticles [33], as well as exploring the upper limit of the size of cargo. In addition, the use of more stable analogies of neurotensin will be explored to enhance the translation of these findings to the clinical environment.

Acknowledgements

The authors are grateful to the School of Life Sciences, University of Lincoln - JLB was supported by a fee-waiver MSc scholarship also consumables were funded as part of a pump-priming award and further financial support was received from the School of Life and Health Sciences, Aston University.

References

[1] S.V. Gudkov et al., Targeted radionuclide therapy of human tumors, Int. J. Mol. Sci. 17 (1) (2016).
[2] A. Accardo et al., Receptor binding peptides for target-selective delivery of nanoparticles encapsulated drugs, Int. J. Nanomed. 9 (2014) 1537–1557.
[3] W.C. Mustain, P.G. Rychahou, B.M. Evers, The role of neurotensin in physiologic and pathologic processes, Curr. Opin. Endocrinol. Diabetes Obes. 18 (1) (2011) 75–82.
[4] J. Mazella, J.P. Vincent, Internalization and recycling properties of neurotensin receptors, Peptides 27 (10) (2006) 2488–2492.
[5] S. Dupouy et al., The potential use of the neurotensin high affinity receptor 1 as a biomarker for cancer progression and as a component of personalized medicine in selective cancers, Biochimie 93 (9) (2011) 1369–1378.
[6] Z. Wu et al., Neurotensin and its high affinity receptor 1 as a potential pharmacological target in cancer therapy, Front. Endocrinol. (Lausanne) 3 (2012) 184.
[7] C. Falciani et al., Synthesis and biological activity of stable branched neurotensin peptides for tumor targeting, Mol. Cancer Ther. 6 (9) (2007) 2441–2448.
[8] C. Falciani et al., Modular branched neurotensin peptides for tumor target tracing and receptor-mediated therapy: a proof-of-concept, Curr. Cancer Drug Targets 10 (7) (2010) 695–704.
[9] Y. Jia et al., Evaluation of DOTA-chelated neurotensin analogs with spacer-enhanced biological performance for neurotensin-receptor-1-positive tumor targeting, Nucl. Med. Biol. 42 (11) (2015) 816–823.
[10] P. Antunes et al., Influence of different spacers on the biological profile of a DOTA-somatostatin analogue, Bioconjug. Chem. 18 (1) (2007) 84–92.
[11] C. Falciani et al., Target-selective drug delivery through liposomes labeled with oligobranched neurotensin peptides, ChemMedChem 6 (4) (2011) 678–685.
[12] J. Brunetti et al., Neurotensin branched peptide as a tumor-targeting agent for human bladder cancer, Biomed. Res. Int. 2015 (2015) 173507.
[13] C. Falciani et al., Nanoparticles exposing neurotensin tumor-specific drivers, J. Pept. Sci. 19 (4) (2013) 198–204.
[14] C. Falciani et al., Cancer selectivity of tetrabranched neurotensin peptides is generated by simultaneous binding to sulfated glycosaminoglycans and protein receptors, J. Med. Chem. 56 (12) (2013) 5009–5018.
[15] P. Kitabgi, Functional domains of the subtype 1 neurotensin receptor (NTS1), Peptides 27 (10) (2006) 2461–2468.
[16] C. Granier et al., Synthesis and characterization of neurotensin analogues for structure/activity relationship studies. Acetyl-neurotensin-(8–13) is the shortest analogue with full binding and pharmacological activities, Eur. J. Biochem. 124 (1) (1982) 117–124.

[17] J.M. Backer, C.R. Kahn, M.F. White, The dissociation and degradation of internalized insulin occur in the endosomes of rat hepatoma cells, J. Biol. Chem. 265 (25) (1990) 14828–14835.
[18] F. Vandenbulcke et al., Ligand-induced internalization of neurotensin in transfected COS-7 cells: differential intracellular trafficking of ligand and receptor, J. Cell Sci. 113 (17) (2000) 2963–2975.
[19] E. Garcia-Garayoa et al., In vitro and in vivo evaluation of new radiolabeled neurotensin(8–13) analogues with high affinity for NT1 receptors, Nucl. Med. Biol. 28 (1) (2001) 75–84.
[20] E. Garcia-Garayoa et al., Preclinical evaluation of a new, stabilized neurotensin (8–13) pseudopeptide radiolabeled with (99 m)tc, J. Nucl. Med. 43 (3) (2002) 374–383.
[21] E. Moroz, S. Matoori, J.C. Leroux, Oral delivery of macromolecular drugs: where we are after almost 100 years of attempts, Adv. Drug Deliv. Rev. 101 (2016) 108–121.
[22] B. Srinivasan et al., TEER measurement techniques for in vitro barrier model systems, J. Lab. Autom. 20 (2) (2015) 107–126.
[23] A.A. Stepanenko, V.V. Dmitrenko, HEK293 in cell biology and cancer research: phenotype, karyotype, tumorigenicity, and stress-induced genome-phenotype evolution, Gene 569 (2) (2015) 182–190.
[24] C.A. Bailey, P. Bryla, A.W. Malick, The use of the intestinal epithelial cell culture model, Caco-2, in pharmaceutical development, Adv. Drug Deliv. Rev. 22 (1–2) (1996) 85–103.
[25] B.K. Atwood et al., Expression of G protein-coupled receptors and related proteins in HEK293, AtT20, BV2, and N18 cell lines as revealed by microarray analysis, BMC Genomics 12 (2011) 14.
[26] M. Mendez et al., High affinity neurotensin receptor mRNA distribution in rat brain and peripheral tissues. Analysis by quantitative RT-PCR, J. Mol. Neurosci. 9 (2) (1997) 93–102.
[27] V.S. Seybold et al., Neurotensin binding sites in porcine jejunum: biochemical characterization and intramural localization, Synapse 6 (1) (1990) 81–90.
[28] K.V. Grunddal et al., Neurotensin is coexpressed, coreleased, and acts together with GLP-1 and PYY in enteroendocrine control of metabolism, Endocrinology 157 (1) (2016) 176–194.
[29] S.F. Cai et al., Differentiation-dependent expression and localization of the class B type I scavenger receptor in intestine, J. Lipid Res. 42 (6) (2001) 902–909.
[30] V.S. Subramanian et al., Differentiation-dependent regulation of intestinal vitamin B(2) uptake: studies utilizing human-derived intestinal epithelial Caco-2 cells and native rat intestine, Am. J. Physiol. Gastrointest. Liver Physiol. 304 (8) (2013) G741–G748.
[31] Y. Konishi, K. Hagiwara, M. Shimizu, Transepithelial transport of fluorescein in Caco-2 cell monolayers and use of such transport in in vitro evaluation of phenolic acid availability, Biosci. Biotechnol. Biochem. 66 (11) (2002) 2449–2457.
[32] D. Vllasaliu et al., Fc-mediated transport of nanoparticles across airway epithelial cell layers, J. Control Release 158 (3) (2012) 479–486.
[33] R. Fowler et al., Nanoparticle transport in epithelial cells: pathway switching through bioconjugation, Small 9 (19) (2013) 3282–3294.